# Characterization of the α-Helix Region in Domain 3 of the Haemolytic Lectin CEL-III: Implications for Self-Oligomerization and Haemolytic Processes

**Keigo Hisamatsu, Nobuaki Tsuda, Shuichiro Goda and Tomomitsu Hatakeyama***

*Department of Applied Chemistry, Faculty of Engineering, Nagasaki University, Bunkyo-machi 1-14, Nagasaki 852-8521, Japan*

**CEL-III is a haemolytic lectin, which has two β-trefoil domains (domains 1 and 2) and a β-sheet-rich domain (domain 3). In domain 3 (residues 284–432), there is a hydrophobic region containing two α-helices (H8 and H9, residues 317–357) and a loop between them, in which alternate hydrophobic residues, especially Val residues, are present. To elucidate the role of the α-helix region in the haemolytic process, peptides corresponding to different parts of this region were synthesized and characterized. The peptides containing the sequence that corresponded to the loop and second α-helix (H9) showed the strongest antibacterial activity for *Staphylococcus aureus* and *Bacillus subtilis* through a marked permeabilization of the bacterial cell membrane. The recombinant glutathione S-transferase (GST)-fusion proteins containing domain 3 or the α-helix region peptide formed self-oligomers, whereas mutations in the alternate Val residues in the α-helix region lead to decreased oligomerization ability of the fusion proteins. These results suggest that the α-helix region, particularly its alternate Val residues are important for oligomerization of CEL-III in target cell membranes, which is also required for a subsequent haemolytic action.**

**Key words: antibacterial peptide, Ca²⁺-dependent lectin, haemolysin, oligomerization, small-angle X-ray scattering.**

Abbreviations: CD, circular dichroism; SAXS, small-angle X-ray scattering; GST, glutathione S-transferase; TBS, Tris-buffered saline; TSB, tryptic soy broth; PBS, phosphate-buffered saline.

CEL-III is one of the $Ca^{2+}$-dependent, Gal/GalNAc-specific lectins isolated from the sea cucumber *Cucumaria echinata* (*1*). CEL-III exhibits strong haemolytic and cytotoxic activity through formation of oligomeric ion-permeable pores in the cell membrane, after binding to cell surface carbohydrate chains (*2–4*). From X-ray crystallographic analysis (*5*), CEL-III was found to consist of three domains (Fig. 1). Domains 1 and 2 are ricin-type (R-type) lectin domains (*6*), also known as β-trefoil domains, having carbohydrate-binding activity, while domain 3 has a novel structure composed of extended β-sheets and two α-helices positioned nearly perpendicular to the β-strands. Limited digestion of CEL-III with trypsin resulted in cleavage between these domains, followed by self-oligomerization of domain 3 fragments (*7*). This result suggested that domain 3 plays an important role in association of CEL-III molecules through interaction between its hydrophobic region, once separated from other domains. It seems that a conformational change induced by binding to carbohydrate chains on the target cell surface may lead to exposure of the hydrophobic surface of domain 3 of CEL-III.

We have previously revealed that some 20-mer synthetic peptides corresponding to the α-helix region that spans α-helices H8 and H9 (residues 320–354) of CEL-III (Fig. 1) exhibited antibacterial activity toward two Gram-positive bacteria *Staphylococcus aureus* and *Bacillus subtilis* (*8*). This activity was assumed to be due to perturbation of cell membranes caused by these peptides, since there was a marked increase in permeability of natural as well as synthetic lipid membranes to small molecules. The α-helix region of CEL-III is the most hydrophobic region of the molecule (*9*) and contains characteristic alternate hydrophobic sequences including two clusters of Val residues (residues 322–326 and 341–345). Such alternate sequences of hydrophobic and hydrophilic residues are often found in β-hairpin regions of pore-forming bacterial toxins that can be inserted into target cell membranes to form membrane-penetrating β-barrel structures (*10*). Therefore, it seems possible that the α-helix region of CEL-III could also play a similar role in the formation of pores in the target cell membrane.

In the present study, we have investigated properties of the α-helix region in domain 3 to elucidate its role in the oligomerization and haemolytic action of CEL-III. Results from synthetic peptides and GST-fusion proteins suggest that the α-helix region, especially its alternate hydrophobic residues, is important in self-oligomerization of domain 3, probably through a large structural transition from α-helix to β-sheet.

*To whom correspondence should be addressed. Tel: +81-95-819-2686, Fax: +81-95-819-2684, E-mail: thata@nagasaki-u.ac.jp
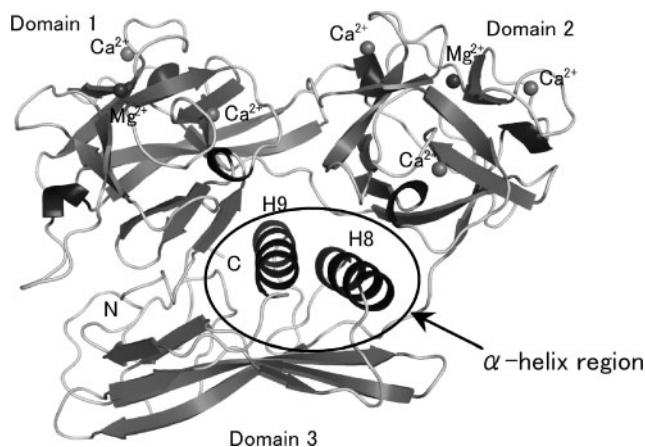
Fig. 1. **Three-dimensional structure of CEL-III determined by X-ray crystallographic analysis (5) (PDB code, 1VCL).** Two α-helices in domain 3 are indicated as 'H8' and 'H9'.

Table 1. **PCR primers for DNA fragment amplification corresponding to domain 3, the α-helix region, and its mutants.**

| Amplified region | Primer | Nucleotide sequence |
|---|---|---|
| Domain 3 | D3-F | 5′-GGATCCTCTTCCACGGTG ACAGCGGGAGTG-3′ |
| | D3-R | 5′-GGATCCTCATGTTCCTGAT TGGCTATTGGTCCA-3′ |
| α-Helix region | HLH-F | 5′-GGATCCTCAAATGTCCGTG CAGAAGTGCA-3′ |
| | HLH-R | 5′-GGATCCTCAAATGTCCGTG CAGAAAG-3′ |
| Mutants of α-helix region (HLH-VA1, HLH-VA2 and HLH-VA3) | HLH-VA-F | 5′-ATTTTTGCCAAAGCGGAAG CGGGCGCGAAAGCGTCAGC CTCGTTGTCTAAAGCATGGA CCAATAGCCAATCAGGAAC ATGAGGATCC-3 |
| | HLH-VA-R | 5′-GGATCCTCATGTTCCTGA TTGGCTATTGGTCCATGCTT TAGACAACGAGGCTGACGCT TTCGCGCCCGCTTCCGCTT TGGCAAAAAT-3′ |

## MATERIALS AND METHODS

*Peptide Synthesis*—Peptides corresponding to the α-helix region sequences (HLH, HL, LH and P332) were synthesized by the solid-phase method using Fmoc-amino acids and 4-(2′,4′-dimethoxyphenylaminomethyl)phenoxy resin (TGR resin) (*11*). Protecting groups and resin were removed with TFA in the presence of *m*-cresol (2%) and thioanisole (12%) at room temperature for 60 min. Crude peptides were precipitated with diethylether on ice, and then purified by reverse-phase HPLC on a Wakosil 5C4 column (Wako, Osaka, Japan). Amino acid sequences of the resulting peptides were confirmed with a PPSQ-21 protein sequencer (Shimadzu, Kyoto, Japan).

*Circular Dichroism (CD) Spectroscopy*—Far-UV CD spectra of peptides were recorded using a J-720 spectropolarimeter (JASCO, Tokyo, Japan). Spectra were measured using a quartz cell with a 1-mm path length at 20°C at a peptide concentration was 0.1 mM.

*Measurement of Peptide Antibacterial Activity*—Antibacterial activity was measured by the serial solution dilution method as previously described (*12*), using two Gram-positive bacteria (*Staphylococcus aureus* IFO 12732 and *Bacillus subtilis* IFO 3134). Each cell suspension was diluted to $10^4$ cells/mL with tryptic soy broth (TSB) medium (pH 7.4). Various concentrations of each peptide solution (10 μL) were placed in a 96-well microplate and 90 μL aliquots of the cell suspension in TSB were added. After incubation for 6 h at 37°C, growth of the bacteria was expressed as turbidity as measured by absorbance at 620 nm using a microplate reader.

*Measurement of Inner Membrane Permeabilization*—The inner membrane permeability of bacterial cells was determined using *o*-nitrophenyl-β-D-galactopyranoside (ONPG) (*13*). Bacteria grown to logarithmic phase were adjusted to $A_{600} = 0.5$ with TSB and mixed with two volumes of 10 mM sodium phosphate buffer, pH 7.4. To this solution (0.8 mL), 0.1 mL of peptides (0.2 mM) and 0.1 mL of ONPG (25 mM) in phosphate-buffered saline (PBS) were added. The inner membrane permeability was monitored as the production of *o*-nitrophenol, as measured by absorbance at 420 nm.

*Preparation of Liposomes*—Egg phosphatidylcholine (5 μmol) was dissolved in $CHCl_3/CH_3OH$ (2:1 (v/v), 0.4 mL), and then dried under a stream of $N_2$ gas. Dried lipid was hydrated in 10 mM Tris–HCl (pH 7.5) containing 0.15 M NaCl (TBS) using a bath-type sonicator. The suspension was sonicated for 10 min at 50°C using a probe sonicator. Liposomes were allowed to stand for 30 min at 25°C before measurements were made. Lipid concentration was 1 mM. Vesicles containing carboxyfluorescein were similarly prepared by hydrating dried lipid in TBS containing 0.1 M carboxyfluorescein. Vesicles containing carboxyfluorescein were separated from free dye by gel filtration using Sephadex G-75 (1 × 22 cm) in TBS.

*Measurement of Carboxyfluorescein-Leakage from Liposomes*—Liposome solution was diluted to 990 μL with TBS and placed in a quartz cuvette kept at 25°C. Peptide solution (10 μL) in the same buffer was added to this solution and, after mixing, solution was excited at 490 nm and fluorescence intensity was immediately recorded at 518 nm for an appropriate period using a Hitachi F-3010 Fluorescence Spectrophotometer. For 100% leakage of carboxyfluorescein, Triton X-100 was added to a final concentration of 0.1% (v/v) and fluorescence intensity was measured.

*Expression of GST-Fusion Proteins Containing the Entire Domain 3 and the α-Helix Region*—Two sets of forward and reverse primers for PCR (Table 1) were used to amplify the DNA corresponding to the entire domain 3 (D3, residues 284–432) and the α-helix region (HLH, residues 317–357) as shown in Fig. 2. Resulting DNA fragments were cloned into *Escherichia coli* JM109 using the pGEM-T vector (Promega), and their nucleotide sequences were confirmed with a Hitachi DNA Sequencer SQ5500E. Inserted DNA fragments were digested with *Bam*HI, and ligated with the pGEX-4T-1 vector (GE Healthcare) previously digested with the same enzyme. The resulting plasmids containing genes corresponding to the α-helix region and domain 3 were

*J. Biochem.*

Fig. 2. **The positions of PCR primers for amplification of different portions of domain 3 and the α-helix region.** The 5′ to 3′ direction of primers is indicated by arrows.

used for transformation of *E. coli* BL21. These cells were grown in LB broth containing 100 μg/mL ampicillin. After $A_{600}$ reached 0.6, IPTG (final concentration of 0.4 mM) was added to induce the protein. The cells were incubated at 30°C for an additional 5 h, and harvested by centrifugation. The cell pellet was resuspended in TBS and cells were lysed thoroughly by sonication and PMSF was added to a final concentration of 1 mM to inhibit protease activity. The mixture was shaken for 30 min at room temperature and centrifuged at 10,000 rpm for 10 min. The supernatant containing the fusion protein was applied directly onto a glutathione-Sepharose 4B column (1 × 1 cm) and the column was washed with TBS. Bound GST fused with the α-helix region (GST-HLH) and the entire domain 3 (GST-D3) were eluted with 50 mM Tris–HCl, pH 8.0, containing 10 mM reduced glutathione. The resulting GST-fusion proteins were further purified by gel filtration using a Sephacryl S-200 column (2.5 × 60 cm).

*Expression and Purification of GST-HLH Mutant Proteins*—Amplification of genes coding for the mutant α-helix region, HLH-VA1, HLH-VA2 and HLH-VA3, was done by PCR using the following combination of the oligonucleotides, HLH-VA-F/HLH-R, HLH-F/HLH-VA-R and HLH-VA-F/HLH-VA-R (Table 1 and Fig. 2). Amplified DNA fragments were cloned using pGEM-T vector in *E. coli* JM109. The resulting DNA fragments were digested with *Bam*HI, and then ligated with the pGEX-4T-1 vector. Plasmids containing the genes for GST-HLH mutants (GST-HLH-VA1, GST-HLH-VA2, GST-HLH-VA3) were used for transformation of *E. coli* BL21. Expression and purification of the mutant proteins was done by the same method as for GST-HLH.

*Small-Angle X-Ray Scattering (SAXS)*—SAXS measurements were carried out using the optics and detector system installed at beamline BL-10C of the 2.5 GeV-storage ring at the Photon Factory (Tsukuba, Japan). The circulating electron current in the storage ring was 300 to 400 mA. A wavelength (λ of 1.488 Å) was used and the specimen-to-detector distance was about 90 cm. All measurements were carried out at 25°C using a temperature-controlled cell holder. The time for SAXS analysis of GST-D3 solutions (concentration 0.5 to 2 mg/mL) was 1800 s for each measurement, and scattering data from multiple measurements were accumulated for up to 3900 s to improve the signal to noise ratio. Scattering data in different solutions were corrected for attenuation of the incident synchrotron X-ray flux by monitoring the beam with an ionization chamber placed in front of the temperature-controlled specimen chamber.



Fig. 3. **Sequences of the peptides HLH, HL, LH and P332, corresponding to different parts of the α-helix region.** Hydrophobic amino acids are enclosed in boxes. Secondary structures are indicated by horizontal bars with their designations.

A detailed description of SAXS measurements is provided elsewhere (*14*).

The net scattering intensities were obtained by subtracting the values for the blank buffer. The radius of gyration, $Rg,z$, and forward scattered intensity were normalized with respect to the protein concentration. $J(0)/C$, was determined using Guinier's approximation (*15*), log $J(Q)$ vs $Q^*Q$. The weight average molecular weight, $Mw,w$, was determined by referring to $J(0)/C$ of bovine serum albumin and bovine thyroid thyroglobulin.

RESULTS

*Structure and Properties of Synthetic Peptides*—We have previously found that 20-mer peptides derived from the amino acid sequence of the α-helix region in CEL-III, especially peptide P332 (residues 332–351) (Fig. 3), exhibited strong antibacterial activity due to ion-channels formed by the peptides in the cell membrane (*8*). This suggests that the α-helix region plays an important role in the haemolytic action by facilitating the interaction of CEL-III with the target cell membrane. To further characterize this α-helix region, we have synthesized three additional peptides, HLH (residues 317–357), HL (residues 317–336) and LH (residues 328–357). As shown in Fig. 3, these peptides span different portions of the two α-helices (H8 and H9) and the loop region (L) between these two α-helices. To examine the secondary structure of these peptides, their far-UV CD spectra were measured. As shown in Fig. 4A, HL showed a definite β-sheet structure spectrum with a broad negative peak around 216 nm in TBS, while LH and HLH showed spectra with smaller negative peaks around 210–220 nm. However, after addition of the liposomes composed of neutral lipids (egg phosphatidylcholine), negative peaks of LH and HLH increased, indicating that the interaction with lipid membrane promoted β-sheet formation of these peptides (Fig. 4B). On the contrary, the negative HL
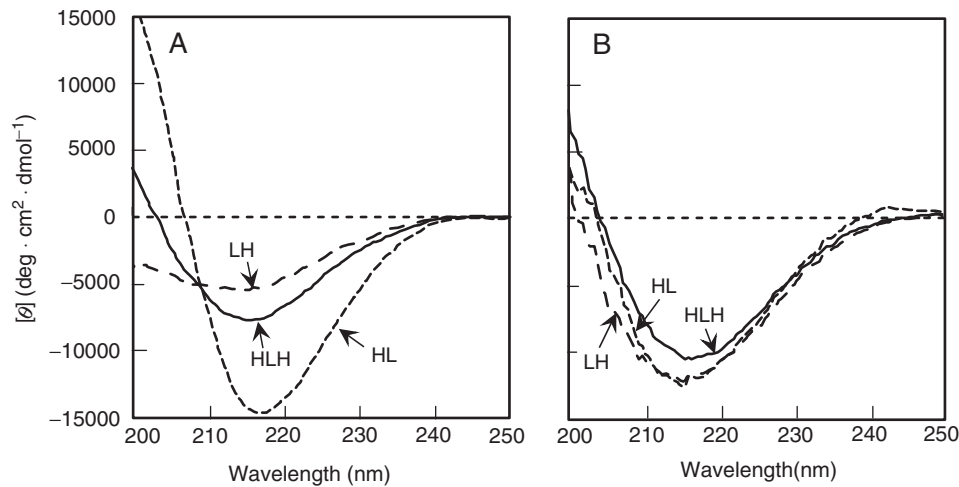
Fig. 4. **Far-UV CD spectra of peptides.** Spectra of the synthetic peptides HLH, HL and LH were measured in TBS (A) or in TBS containing 1 mM egg phosphatidylcholine liposomes (B).

peak around 216 nm slightly decreased after addition of liposomes. This indicates that HL has the strongest tendency to form β-sheet among these peptides in solution, which cannot be promoted by the interaction with lipid membrane.

In order to examine the effect of the synthetic peptides on bacterial cell membranes, they were incubated with bacterial cells at 37°C for 6 h and turbidity of the solution was measured as an indication of bacterial growth. As shown in Table 2, of the examined peptides, HLH exhibited the highest antibacterial activity against the Gram-positive bacteria, *S. aureus* and *B. subtilis*, which was comparable to peptide P332. This was followed by LH, whereas little inhibition of bacterial growth was observed with HL. The membrane permeabilizing ability of these peptides was examined using ONPG, a chromogenic substrate for cytosolic β-galactosidase. Hydrolysis of internalized ONPG was detected by measuring the absorbance at 420 nm, which reflects the permeabilization of the inner cell membrane (*13*). As shown in Fig. 5, HLH, P332, and LH exhibited effective permeabilization of the bacterial membrane in this order, while HL induced only a small increase in membrane permeabilization. Ion channel formation in artificial lipid membranes by these peptides was confirmed by the carboxyfluorescein (CF)-leakage assay using CF-trapping liposomes. Figure 6 shows the effect of the peptides on egg phosphatidylcholine-liposomes containing CF. When liposomes were incubated with the peptides, higher CF-leakage was observed with HLH, P332 and LH, whereas HL exhibited CF-leakage to a much lesser extent. These results confirmed that α-helix region peptides, especially those containing the loop and H9 regions, have the ability to form ion channels in the membrane. The formation of these ion channels in the membrane has an obvious relationship with antibacterial activity.

*Expression of GST-Fusion Proteins Containing the Entire Domain 3 of CEL-III and the α-Helix Region Peptides*—Domain 3 has been shown to have a tendency to oligomerize spontaneously, once cleaved from the intact protein by limited digestion with proteases, such

Table 2. **Antibacterial activity of peptides corresponding to the α-helix region of CEL-III.**

| Peptide | Minimum inhibitory concentration to inhibit bacterial growth (μM) | |
|---|---|---|
| | *S. aureus* | *B. subtilis* |
| HL | >50 | >50 |
| LH | 12 | 12 |
| HLH | 3 | 6 |
| P332 | 3 | 6 |
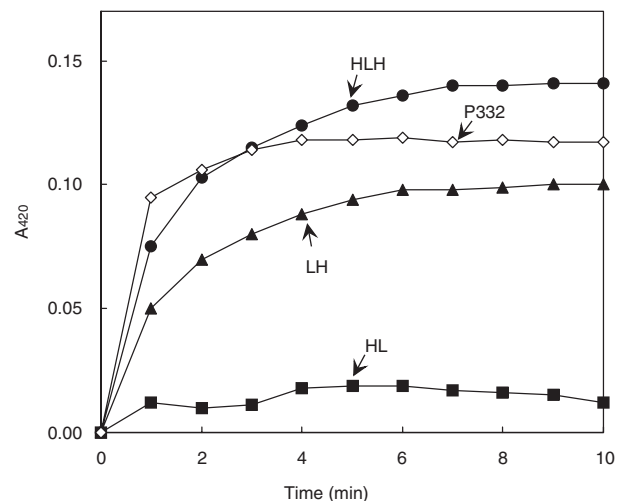


Fig. 5. **Permeabilization of the inner membrane of *S. aureus* induced by the synthetic peptides.** Bacterial cells were incubated with peptides (0.5 mM) and ONPG (2.5 mM) at 37°C and the production of *o*-nitrophenol due to the increasing permeability of the inner cell membrane was monitored by the absorbance at 420 nm.

as trypsin and chymotrypsin (*7*); strongly suggesting that domain 3 is primarily responsible for self-oligomerization of CEL-III in the target cell membranes. To characterize the oligomerizing ability of domain 3, focusing on the
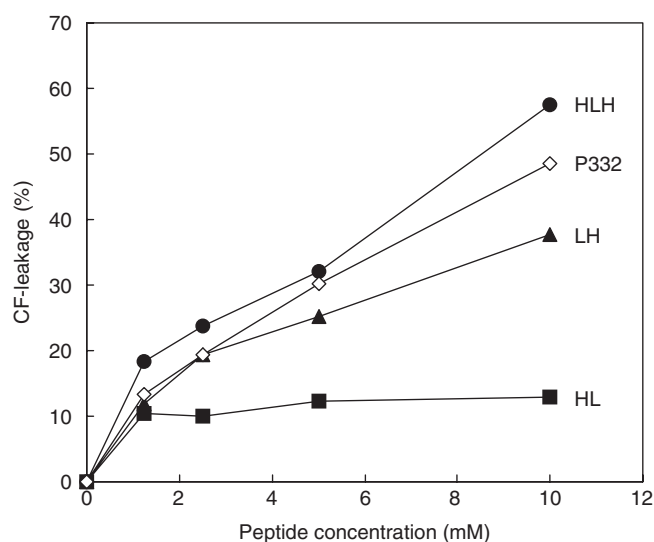
Fig. 6. **CF-leakage assay of the synthetic peptides using egg phosphatidylcholine liposomes.** Peptides were incubated with the liposomes trapping 0.1 M carboxyfluorescein in TBS, and the increase in fluorescence intensity at 518 nm arising from the leakage of carboxyfluorescein was measured with an excitation wavelength of 490 nm. The fluorescence intensity after the addition of 0.1% Triton X-100 was taken as a 100% leakage.



Fig. 7. **Gel filtration of GST (A) and GST-fusion proteins containing the entire domain 3 (GST-D3) (B) or the α-helix-region peptide (GST-HLH) (C).** The proteins were applied on a column of Sephacryl S-200 ($2.5 \times 60\,cm^2$) in TBS.

Table 3. **Structural parameters of GST-D3 and CEL-III oligomer determined by SAXS.**

| Protein | $Rg,z$ (Å) | $D_{max}$ (Å) | $M$w,w(kDa) | $M$w of monomer (kDa) |
|---|---|---|---|---|
| GST-D3 | $98.2 \pm 1.8$ | 250 | 1050 | 43 |
| CEL-III[a] | $101.4 \pm 1.0$ | 290 | 1019 | 47 |

The radius of gyration, $Rg,z$, which is given by the least squares fit of the linear region of a Guinier plot (*15*), reflects the molecular shape and size. Forward scattering intensity, $J(0)$, normalized to the protein concentration $C$, $J(0)/C$, is proportional to the weight average molecular weight $M$w,w (*22*), while $D_{max}$ obtained from the $p(r)$ function, which is the Hankel transform of the scattering curve, gives the maximum particle dimension ($D_{max}$).
[a]Values previously reported in (*19*).

involvement of the α-helix region, GST-fusion proteins that contained the HLH peptide (GST-HLH) or the entire domain 3 (GST-D3) were expressed in *E. coli* cells. Expressed proteins were obtained in soluble form after disruption of the cells, and further purified using glutathione-Sepharose 4B and gel-filtration columns. As shown in the elution profile of the gel filtration on the Sephacryl S-200 column (Fig. 7), while GST, which spontaneously formed dimer (53.5 kDa) (*16*), was eluted at 88 min (A), the fusion proteins GST-D3 (B) and GST-HLH (C) were eluted around 60 min, which was much earlier than expected from their molecular masses (GST-D3 dimer, 84.8 kDa; GST-HLH dimer, 61.8 kDa). This result indicated that domain 3 of CEL-III, especially its α-helix region, has a strong tendency to self-associate leading to formation of oligomers, even when fused to the unrelated protein.

*SAXS Measurement of the GST-D3 Oligomer*—In order to determine the size of the GST-D3 oligomer, SAXS measurements were carried out using synchrotron radiation and the obtained values are summarized in Table 3. The measurements were done using a range of 0.5 to 2.0 mg/mL of protein to confirm the effect of protein concentration. The concentration dependency of $Rg,z$ due to inter-particle interaction was negligible (data not shown). The $Rg,z$ and $D_{max}$ value of GST-D3 was 98.2 and 250 Å, respectively. The $M$w,w value of GST-D3 was 1,050 kDa, which corresponds to a 24-mer of GST-D3.

*Expression of GST-HLH Mutants*—The α-helix region of CEL-III contains alternate hydrophobic and hydrophilic amino acid residues and resembles the membrane-associating β-strand region of several pore-forming bacterial toxins, such as α-haemolysin from *Staphylococcus aureus* (Fig. 8) (*10*). Interestingly, there are two characteristic Val clusters in the α-helix region of CEL-III, in which three Val residues are aligned at every second position (Fig. 8A). Therefore, focusing on the role of these Val residues, we prepared three mutants of GST-HLH, in which these different Val residues were replaced by Ala (GST-HLH-VA1, GST-HLH-VA2 and GST-HLH-VA3) (Fig. 9). The elution profiles of these mutants on the Sephacryl S-200 column are shown in Fig. 10. Although GST-HLH that contained the wild-type sequence mostly formed oligomers, replacement of Val
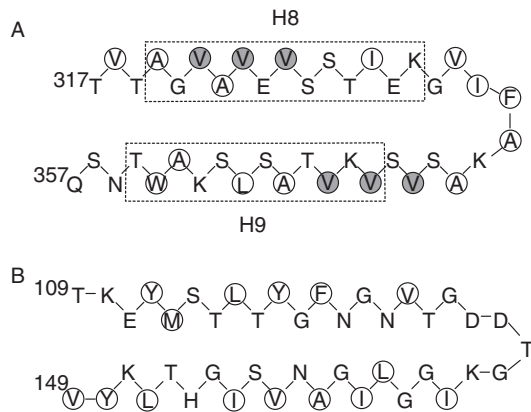
Fig. 8. **Amino acid sequence of the α–helix region of CEL-III (A) compared to the membrane binding region of α-haemolysin from *S. aureus* (B).** Hydrophobic amino acid residues are enclosed in circles, of which three consecutive Val residues at every second position (residues 322–326 and 341–345) are indicated by shading. Amino acid residues composing the two α-helices (H8 and H9) are indicated by dotted boxes.
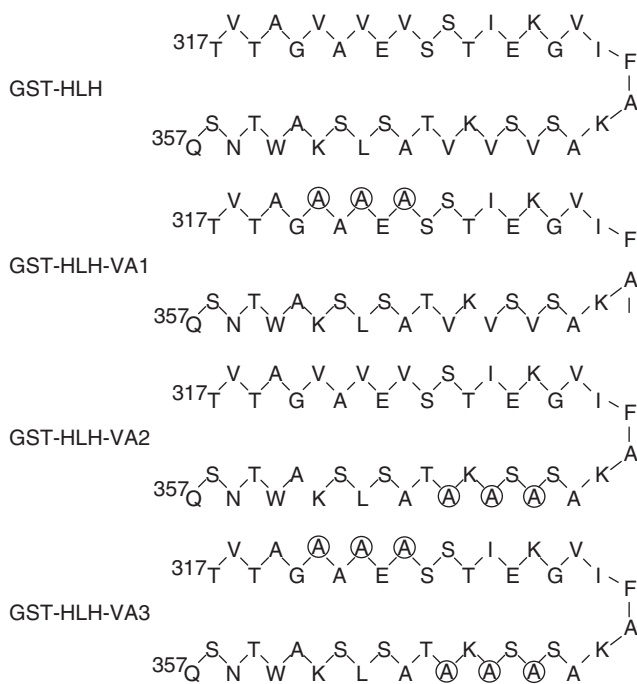


Fig. 9. **Amino acid sequence of GST-HLH and its Val-substituted mutants (GST-HLH-VA1, GST-HLH-VA2 and GST-HLH-VA3).** The residues substituted from Val to Ala are enclosed in circles.

to Ala resulted in decreased oligomerization of fusion proteins. These results suggest that the alternate hydrophobic residues, like Val clusters, may have an important role in oligomerization of proteins. In addition, the decrease in oligomerization was more prominent in GST-HLH-VA2 than in GST-HLH-VA1, suggesting that Val residues at positions 341–345 are more important for oligomerization than in positions 322–326.
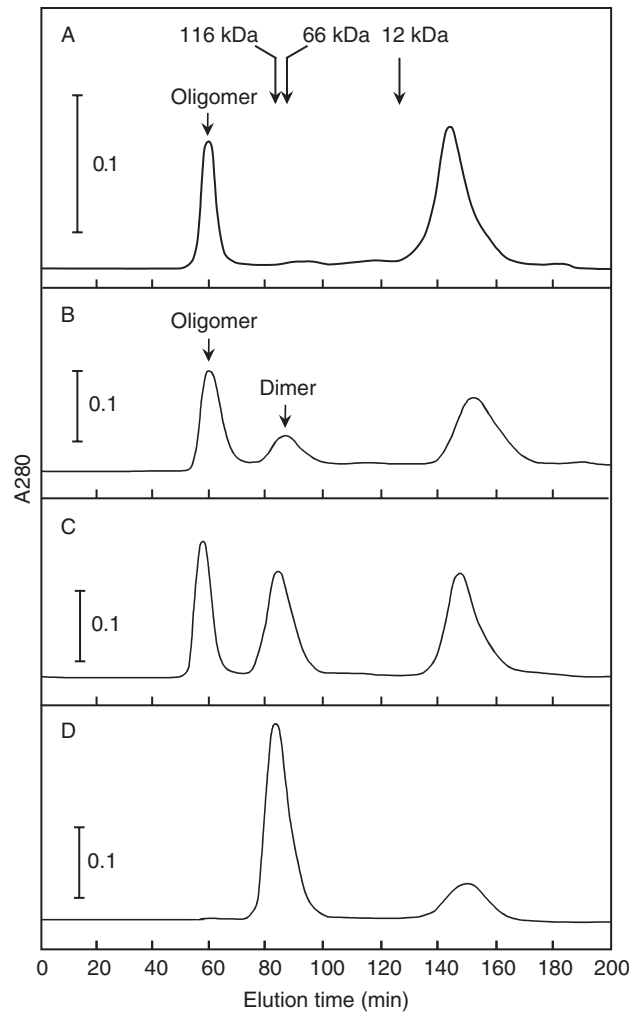


Fig. 10. **Gel filtration of GST-HLH and its mutants.** GST-HLH (A) and its Val-substituted mutants, GST-HLH-VA1 (B), GST-HLH-VA2 (C) and GST-HLH-VA3 (D), were applied on a column of Sephacryl S-200 ($2.5 \times 60$ cm) in TBS. Elution profile of GST-HLH (A) is the same as that in Fig. 7C.

## DISCUSSION

In the current study, three peptides corresponding to different portions of the α-helix region were made in addition to P332, and significant antibacterial and membrane permeabilizing activities were observed with HLH, LH and P332, but not with HL. Although β-sheet contents of the peptides HLH and LH were relatively low in aqueous solution, they increased upon addition of lipid vesicles, suggesting that interaction with lipid membrane induced β-sheet formation in the membrane. In contrast, the peptide HL, which showed the highest β-sheet content in solution, slightly decreased its β-sheet content in the presence of lipid vesicles. Taking these facts into account, it appears that the increase in β-sheets of the peptides upon binding with lipid membrane may be closely related to their antibacterial and membrane permeabilizing activities. One of the possibilities is that after binding to the membrane HLH and LH may

*J. Biochem.*

associate to form ion channels composed of β-sheet structure. Similar observation has also been reported for cationic α-helical peptides; higher antibacterial activity was observed for the peptides, which increased α-helix content upon interaction with lipid membranes, whereas those having strong α-helicity in solution exhibited rather low activity (*17*).

In general, a number of naturally occurring antibacterial peptides exhibit their activity through membrane perturbation by the formation of amphiphilic α-helices in target cell membranes (*18*). These peptides often contain amino acid sequences with periodically occurring hydrophobic and hydrophilic residues at every third or fourth position to form amphiphilic α-helices (*19*). In contrast, the α-helix region of CEL-III has hydrophobic residues at every second position. This suggests that when the α-helix region of CEL-III adopts a β-sheet structure, it forms an amphiphilic β-sheet with hydrophobic and hydrophilic faces on opposite sides, leading to self-oligomerization through hydrophobic interactions.

The importance of the α-helix region in self-oligomerization of CEL-III was confirmed by the finding that GST-D3 and GST-HLH tend to form self-oligomers in solution, as seen in the elution profile of gel filtration on a Sephacryl S-200 column (Fig. 7). The actual size of these oligomers could not be determined by gel filtration, since they eluted at the void volume of the column. However, SAXS measurements of GST-D3 revealed that it has a molecular mass of 1050 kDa, which corresponds to a 24-mer of the monomer protein. Since the molecular mass of the CEL-III oligomer induced after binding of lactose has previously been estimated to be 1,019 kDa by SAXS, corresponding to a 21-mer (*20*), it seems that GST-D3 also associates in a similar manner as intact CEL-III through their domain 3 regions.

One of the characteristic features of the α-helix region in domain 3 is the presence of two Val clusters, in which three consecutive Val residues appear at every second position (residues 322–326 and 341–345). Replacement of these Val residues to Ala residues resulted in a marked decrease of oligomer proteins, as seen in the elution profiles on the Sephacryl S-200 column (Fig. 10). This strongly suggests that Val clusters are important in the self-oligomerization of these proteins.

Amino acid sequences with alternate hydrophobic and hydrophilic residues have also been found in the membrane-inserting β-strand region of several pore-forming toxins (*10*). They associate in target membranes, forming β-barrels. In such membrane-penetrating β-barrels, hydrophobic and hydrophilic residues of the β-sheet face the lipid bilayer and lumen of the pore, respectively, as demonstrated in case of the heptamer structure of α-haemolysin of *Staphylococcus aureus* (*21*). Alternate hydrophobic and hydrophilic residues in the α-helix region of CEL-III suggest that the haemolysis mechanism is similar for CEL-III and bacterial toxins. To form such a β-barrel in the membrane, the α-helix region of CEL-III must undergo drastic conformational changes from α-helices to β-strands. Conformational transitions of proteins from α-helix to β-strand has been attracting much attention, because of its possible involvement in conformational diseases such as Alzheimer's disease, Parkinson's disease and spongiform encephalopathies. Elucidation of the conformational alteration of CEL-III in the course of its haemolytic action would also provide valuable insights into the mechanisms of such conformational diseases.

## REFERENCES

1. Hatakeyama, T., Kohzaki, H., Nagatomo, H., and Yamasaki, N. (1994) Purification and characterization of four Ca$^{2+}$-dependent lectins from the marine invertebrate, *Cucumaria echinata*. *J. Biochem.* **116**, 209–214
2. Oda, T., Tsuru, M., Hatakeyama, T., Nagatomo, H., Muramatsu, T., and Yamasaki, N. (1997) Temperature- and pH-dependent cytotoxic effect of the hemolytic lectin CEL-III from the marine invertebrate *Cucumaria echinata* on various cell lines. *J. Biochem.* **121**, 560–567
3. Hatakeyama, T., Furukawa, M., Nagatomo, H., Yamasaki, N., and Mori, T. (1996) Oligomerization of the hemolytic lectin CEL-III from the marine invertebrate *Cucumaria echinata* induced by the binding of carbohydrate ligands. *J. Biol. Chem.* **271**, 16915–16920
4. Hatakeyama, T., Nagatomo, H., and Yamasaki, N. (1995) Interaction of the hemolytic lectin CEL-III from the marine invertebrate *Cucumaria echinata* with the erythrocyte membrane. *J. Biol. Chem.* **270**, 3560–3564
5. Uchida, T., Yamasaki, T., Eto, S., Sugawara, H., Kurisu, G., Nakagawa, A., Kusunoki, M., and Hatakeyama, T. (2004) Crystal structure of the hemolytic lectin CEL-III isolated from the marine invertebrate *Cucumaria echinata*: implications of domain structure for its membrane pore-formation mechanism. *J. Biol. Chem.* **279**, 37133–37141
6. Rutenber, E. (1991) Structure of ricin B-chain at 2.5 Å resolution. *Proteins* **10**, 260–269
7. Kouzuma, Y., Suzuki, Y., Nakano, M., Matsuyama, K., Tojo, S., Kimura, M., Yamasaki, T., Aoyagi, H., and Hatakeyama, T. (2003) Characterization of functional domains of the hemolytic lectin CEL-III from the marine invertebrate *Cucumaria echinata*. *J. Biochem.* **134**, 395–402
8. Hatakeyama, T., Suenaga, T., Eto, S., Niidome, T., and Aoyagi, H. (2004) Antibacterial activity of peptides derived from the C-terminal region of a hemolytic lectin, CEL-III, from the marine invertebrate *Cucumaria echinata*. *J. Biochem.* **135**, 65–70
9. Nakano, M., Tabata, S., Sugihara, K., Kouzuma, Y., Kimura, M., and Yamasaki, N. (1999) Primary structure of hemolytic lectin CEL-III from marine invertebrate *Cucumaria echinata* and its cDNA: structural similarity to the B-chain from plant lectin, ricin. *Biochim. Biophys. Acta* **1435**, 167–176
10. Leppla, S. (2006) *Bacillus anthracis* toxins, in *The Comprehensive Sourcebook of Bacterial Protein Toxins,* (Alouf, J. and Popof, M., eds.) 3rd edn., pp. 323–347, Academic Press, New York
11. Fields, G.B. (1990) Solid phase peptide synthesis utilizing 9-fluorenylmethoxycarbonyl amino acids. *Int. J. Pept. Protein Res.* **35**, 161–214
12. Yoshida, K., Mukai, Y., Niidome, T., Takashi, C., Tokunaga, Y., Hatakeyama, T., and Aoyagi, H. (2001) Interaction of pleurocidin and its analogs with phospholipid membrane and their antibacterial activity. *J. Pept. Res.* **57**, 119–126
13. Pellegrini, A., Dettling, C., Thomas, U., and Hunziker, P. (2001) Isolation and characterization of four bactericidal domains in the bovine β-lactoglobulin. *Biochem. Biophys. Acta* **1526**, 131–140

14. Hiragi, Y., Seki, Y., Ichimura, K., and Soda, K. (2002) Direct detection of the protein quaternary structure and denatured entity by small-angle scattering: guanidine hydrochloride denaturation of chaperonin protein GroEL. *J. Appl. Cryst.* **35**, 1–7

15. Guinier, A. (1955) *Small-Angle Scattering of X-Rays.* Chapman & Hall, New York

16. Lim, K., Ho, J.X., Keeling, K., Gilliland, G.L., Ji, X., Ruker, F., and Carter, D.C. (1994) Three-dimensional structure of *Schistosoma japonicum* glutathione S-transferase fused with a six-amino acid conserved neutralizing epitope of gp41 from HIV. *Protein Sci.* **3**, 2233–2244

17. Ohmori, N., Niidome, T., Hatakeyama, T., Mihara, H., and Aoyagi, H. (1998) Interaction of α-helical peptides with phospholipid membrane: effects of chain length and hydrophobicity of peptides. *J. Peptide Res.* **51**, 103–109

18. Tossi, A., Sandri, L., and Giangaspero, A. (2000) Amphipathic, α-helical antimicrobial peptides. *Biopolymers* **55**, 4–30

19. Saberwal, G. (1994) Cell-lytic and antibacterial peptides that act by perturbing the barrier function of membranes: facets of their conformational features, structure-function correlations and membrane-perturbing abilities. *Biochim. Biophys. Acta* **1197**, 109–131

20. Fujisawa, T., Kuwahara, H., Hiromasa, Y., Niidome, T., Aoyagi, H., and Hatakeyama, T. (1997) Small-angle X-ray scattering study on CEL-III, a hemolytic lectin from Holothuroidea *Cucumaria echinata*, and its oligomer induced by the binding of specific carbohydrate. *FEBS Lett.* **414**, 79–83

21. Song, L., Hobaugh, M.R., Shustak, C., Cheley, S., Bayley, H., and Gouaux, J.E. (1996) Structure of staphylococcal α-hemolysin, a heptameric transmembrane pore. *Science* **274**, 1859–1866

22. Kajiwara, K. (1996) Structure analysis by small-angle X-ray scattering, in *Applications of Synchrotron Radiation to Material Analysis* (Saisho, H. and Goshi, Y., eds.) Elsevier Science, Amsterdam